Random Telegraph Signal Fluctuations of Dark Count Rate in CMOS SPAD Structures

F. Di Capua, M. Campajola, D. Fiore, C. Nappi, E. Sarnelli

Abstract —**In this paper we report the observation of a peculiar behaviour of Single Photon Avalanche Diode pixels operating in a proton radiation environment.**
The irradiated SPAD cells, in dark environment, start to switch between two or more levels of the Dark Count Rate pedestals. The investigation of main characteristics of such discrete switching makes it attributable to a Random Telegraph Signal phenomenon.
We studied the Dark Count Rate discrete fluctuations as a function of the temperature. The measurements of the time constant of the phenomenon and of corresponding activation energy are reported.

I. Introduction

Single-Photon Avalanche Photodiodes (SPADs) are solid-state sensors with the capability to detect individual photons as well their arrival time with excellent resolution [1].
The implementation of SPADs in CMOS technology [2] has brought this kind of device to a growing interest thanks to the integrated readout and on-chip data processing [3]-[4].
In several fields where single-photon sensitivity and good timing resolution are required, pixel sensors based on SPADs are employed, like vision camera and lidar implementation for space applications [5], in microscopy and biomedical [6] and quantum cryptography [7].
In space and high-energy physics research applications, SPAD devices are often required to operate in a radiation environment. Radiation-induced defects in silicon structure, to which new energy levels in the bandgap are associated, can seriously worsen SPAD performances, since they cause the generation of carriers in depletion regions through both thermal and tunnelling processes [8, 9, 10] by increasing the Dark Count Rate (DCR).
Other than the increase of DCR, the presence of the defects degrades the performance of SPAD devices inducing dark counts discrete fluctuations, known as Random Telegraph Signal (RTS) [11,12]. In this paper we report on the RTS phenomena of two different SPAD structures fabricated in a 150 nm CMOS process after the irradiation with protons. The test chip used contains two layouts: one structure based on P+/Nwell junction enclosed in a low-doped region in order to create a guard-ring to avoid premature edge breakdown; a second structure is constituted by Pwell/Niso junction. More junction details are described in [13-15].

F. Di Capua, M. Campajola are with University of Napoli Federico II, Department of Physics “E. Pancini” and INFN, Napoli, Italy.
D. Fiore is with Università della Calabria, DIMES Department and INFN, Cosenza, Italy.
C. Nappi, E. Sarnelli are with CNR-SPIN Institute, Napoli, Italy

II. The Proton Irradiation

The devices have been irradiated with protons by using a 14 MV Tandem accelerator and a Superconducting Cyclotron (SC) able to accelerate protons up to 62 MeV we irradiated the devices. Both irradiations have been performed at Laboratori Nazionali del Sud (LNS) - Istituto Nazionale di Fisica Nucleare (INFN) in Catania (Italy).
The proton fluence has been measured in line by integrating an ionization chamber current during the whole irradiation time. The ionization chamber has been previously calibrated with a Faraday cup before to irradiate the device. A collimator at the end of beam-line defines the beam shape. The irradiation setup is shown in Fig. 1.

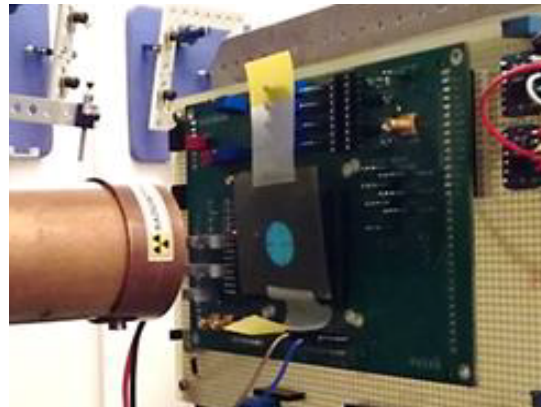

Fig. 1: Test beam setup for SPAD irradiation at LNS Cyclotron;

The dosimetry has been additionally verified with a Gafchromic film EBT3 type [16] positioned at the same position of device under test.. Three samples have been irradiated to similar Displacement Damage Dose (DDD) but with three different proton energies. One sample has been irradiated to a lower DDD of about one third. Direct ionization of protons is responsible for a certain accumulated Total Ionizing Dose (TID) level reported in Tab. 1.

Sample ID	Proton Fluence [p/cm^2]	Energy	TID [krad]	DDD [TeV/g]
1	5.63×10^{10}	21	17.5	376
2	5.60×10^{10}	32	12.5	304
3	7.56×10^{10}	60	10.4	304
4	2.90×10^{10}	60	5.0	115

Table 1: Delivered protons to irradiated samples and corresponding TID and DDD levels.

Previous studies on the same device [17] shown a quite good tolerance to TID up to 1 Mrad, therefore the accumulated TID level during this study can be considered negligible.

III. RTS OBSERVATION

The measurement setup is made by a motherboard providing the power supply to the read-out circuit on chip and the SPAD bias voltage. The output signal is sent to an oscilloscope and to a digital counter. The architecture of the device allows selecting the output of a single SPAD pixel.

The DCR output of each pixel has been acquired for a time of 600 s limiting our research for RTS and time constants at this time scale. The devices have been analysed before the irradiation and two months following the irradiation test to search for the presence of DCR switching pixels.

The measurements of DCR show an increase up to two orders of magnitude, as shown in Figure 2 for a SPAD pixel.

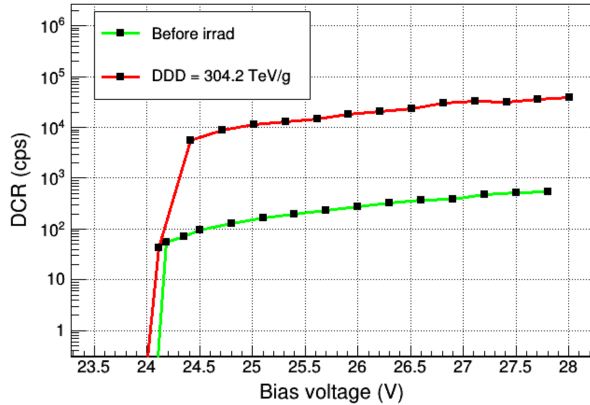

Fig. 2 Dark count rate as a function of applied bias voltage, before and after exposure to displacement damage dose of 304 TeV/g.

After the irradiation a large fraction of pixels in the devices shows RTS behaviour. In Figure 3 the DCR for an irradiated SPAD pixel is plotted as a function of the observation time showing a switching behaviour between two DCR levels. In many other cases the fluctuation of DCR has been found on more than two levels (Fig. 4).

Sometime many levels could be present making difficult to distinguish them. A time lag plot is a scatter plot of data sampled at the *ith* time interval, t_i, versus data sampled at *ith+1* time interval, t_{i+1}. In such kind of plot the RTS levels appear as clusters along the diagonal (Fig. 5).

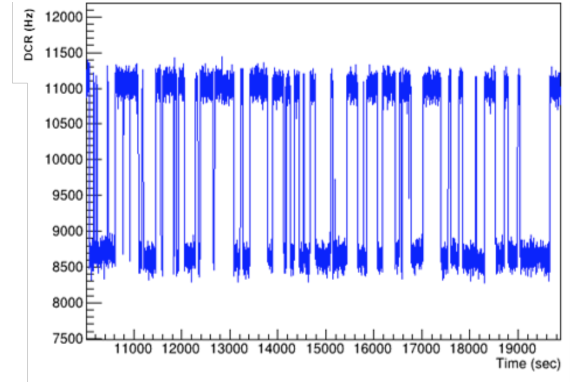

Fig. 3 Two-level DCR fluctuations

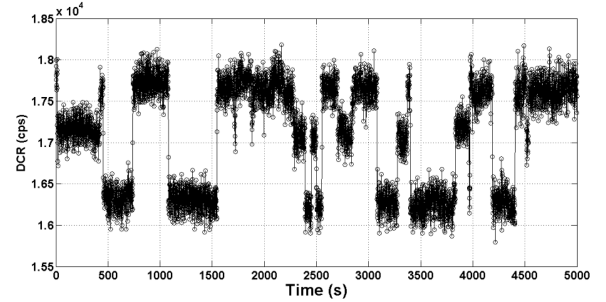

Fig. 4: A three-level RTS in one SPAD pixel

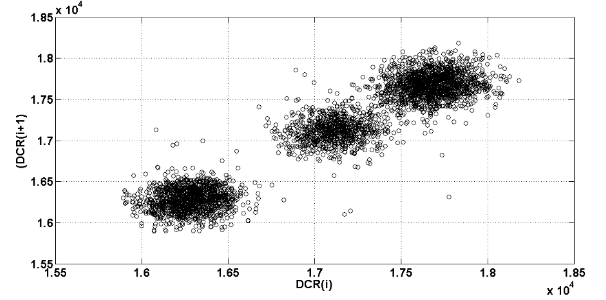

Fig. 5: Time lag plot relative to RTS pixel shown in Fig. 4

Fig 6 shows a SPAD pixel with a switching behaviour between two main levels which seems to be formed by two sub-levels. In the corresponding time lag plot (Fig. 7) the four populations are displayed.

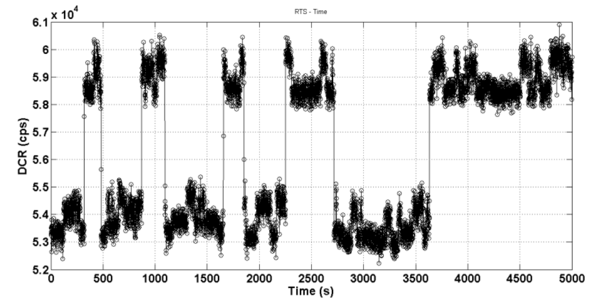

Fig. 6: A four-level RTS in one SPAD pixel: each of two main levels contain two sub-levels

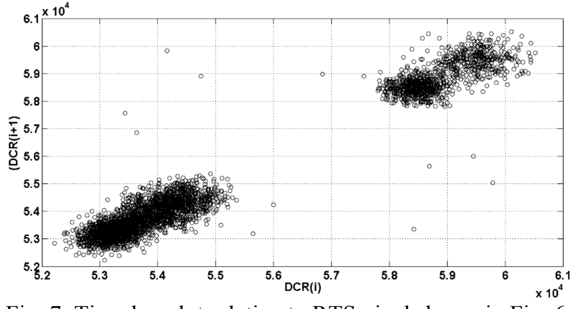

Fig. 7: Time lag plot relative to RTS pixel shown in Fig. 6

In Table 2 the RTS occurrence probability for the irradiated sample n.1 has been reported distinguishing between two, three and multi-level RTS. The analysis proves that two-levels RTS are less probable and the number of RTS pixels with more than two levels is higher, as observed also in [18].
A higher RTS occurrence probability has been observed in P+/Nwell with respect to Pwell/Niso layout.
On a sample of irradiated SPADs with a DDD of 376 TeV/g we observed a fraction of pixel with a RTS behaviour of 85±3% and 58±3% for PN and PWNISO, respectively.

Layout	Analysed SPADs	RTS pixels	2 Levels	3 Levels	Multi Level (>=4)	Total RTS fraction
PN	139	118	17	11	90	85%
PWNISO	321	186	34	15	137	58%

Table 2: Pixels with RTS in two different SPAD layouts for DDD=376 TeV/g

A similar result has been obtained on other two irradiated samples exposed to a DDD of 300 TeV/g but with different proton energy. For a sample exposed to a DDD of 115 TeV/g we observed RTS occurrence fractions 55±5% and 39±3% for PN and PWNISO, respectively (Table 3).

Layout	Analysed SPADs	RTS pixels	2 Levels	3 Levels	Multi Level (>=4)	Total RTS fraction
PN	118	65	18	10	37	55%
PWNISO	334	131	34	9	88	39%

Table 3: Pixels with RTS in two different SPAD layouts for DDD=115 TeV/g

The results indicate that RTS occurrence depends on the accumulated DDD rather than some peculiar energy-dependent proton interaction cross-section.

IV. RTS Characterization

In the following we focused on two-level RTS by investigating in more detail some RTS characteristic. The distribution of times in which the system is in the top (or in bottom) DCR level, follow an exponential distribution (Fig. 8) as foreseen in Poisson distribution of random switching events [19]. The time constants of RTS two-levels have been found to be dependent on the temperature (Fig. 9), namely the switching probability is higher by increasing the temperature. In order to investigate it, continuous DCR measurements on the time scale from few hours up to several days have been performed by varying the temperature from 5°C to 40°C.

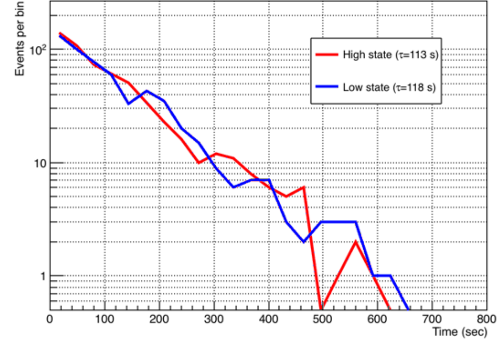

Fig. 8: Time distribution for high and low levels in a SPAD with a two-level RTS fluctuations

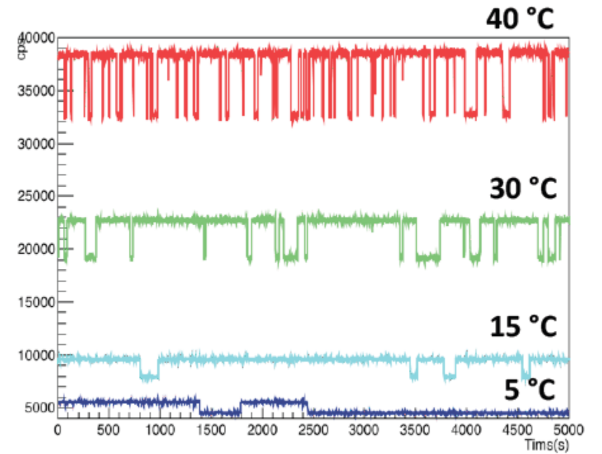

Fig. 9: RTS two-level switching as function of the temperature for a given SPAD pixel

Time constants (τ_{up} and τ_{down}) are seen to vary with temperature according to the law

$$\frac{1}{\tau} = C\exp(-E_{act}/KT)$$

An example of the trend of the measured RTS time constant as a function of the temperature, Fig 12 and Fig 13 show the Arrhenius plot for the high and low DCR levels, respectively. In each graph is reported the measurement of a single two-level RTS found in P+/Nwell and Pwell/Niso layouts.
The values obtained for the time constant activation energy E_{act} are in the range 0.8-1.0 eV and are in agreement with the calculated kinetics of the reorientation of the vacancy relative to phosphorous atom in a P-V center defect [20].
A phosphorus-vacancy center has been already indicated as a possibility to explain RTS behaviour in [21] and [22]. In a phosphorus-doped device, the vacancies created by proton-induced silicon displacement, migrating in the lattice give rise to a P-V center defects (Fig 11).

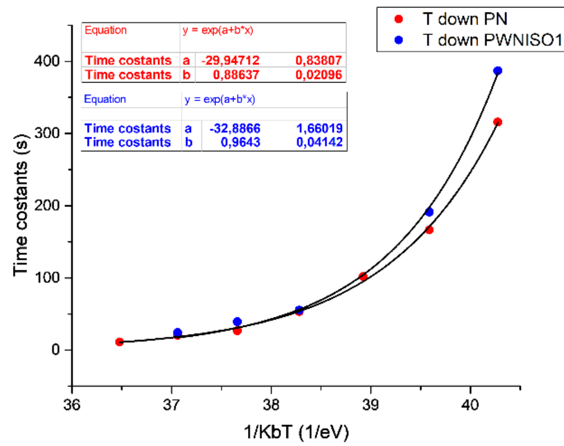

Fig. 9: Time constants as a function of 1/KT for low RTS level in two SPAD pixels with different layouts

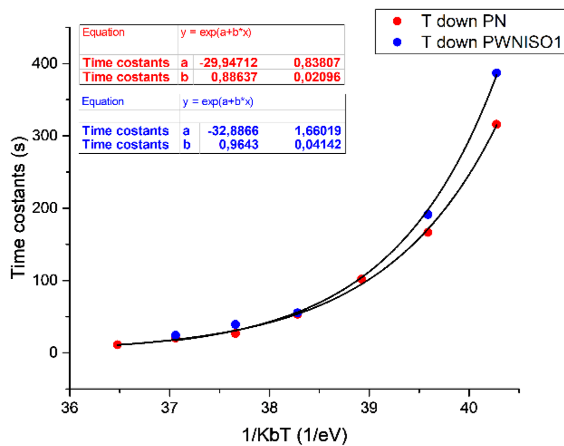

Fig. 10: Time constants as a function of 1/KT for high RTS level in two SPAD pixels with different layouts

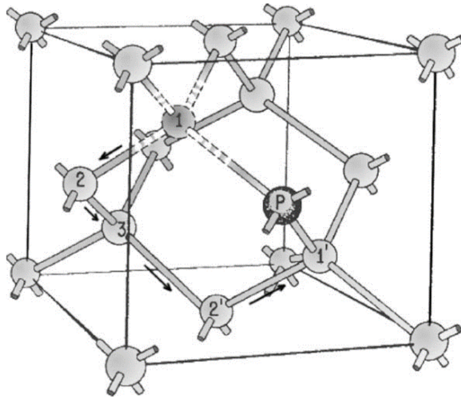

Fig. 11: The silicon lattice containing a P-V center defect

The P-V defect can reorient its axis when the vacancy moves in one of four Si atoms close to P atom. This new position corresponds to a new energy level, which is at the origin of the RTS behaviour.

V. Conclusions

This work reports the RTS observations on two different SPAD layouts, implemented in 150 nm CMOS technology. The devices were irradiated with proton beams of different energies at LNS INFN in Catania.

The RTS measurements reported in this work could support the hypothesis that attributes the RTS behaviour to the reorientation of the phosphorus-vacancy (P-V) center.

The identification of defects responsible of RTS and the understanding of its evolution in different conditions of temperature and bias voltage could be very useful to limit such effect on the devices operating in a radiation environment. Further investigations are certainly necessary to enlarge the knowledge on RTS and to recognize each defects or cluster of defects involved in this mechanism.

References

[1] S. Cova, A. Longoni, and A. Andreoni, "Towards Picosecond Resolution with Single-Photon Avalanche Diodes," *Rev. Sci. Instr.*, vol 52, no. 3, pp. 408- 412, Mar. 1981.

[2] A. Rochas, M. Gani, B. Furrer, P. A. Besse, and R. S. Popovic, G. Ribordy and N. Gisin, Single photon detector fabricated in a complementary metal–oxide–semiconductor high-voltage technology.

[3] F. Zappa, A. Gulinatti, P. Maccagnani, S. Tisa, and S. Cova, "SPADA: Single-photon avalanche diode arrays," IEEE Photon. Technol. Lett., vol. 17, no. 3, pp. 657–659, Mar. 2005

[4] C. Veerappan et al., "A 160 °ø 128 single-photon image sensor with on-pixel 55ps 10b time-to-digital converter," in IEEE Int. Solid-State Circuits Conf. Dig. Tech. Papers (ISSCC), Feb. 2011, pp. 312–314.

[5] B. Aull, "Geiger-Mode Avalanche Photodiode Arrays Integrated to All-Digital CMOS Circuits," Sensors 16(4), 495 (2016).

[6] S. P. Poland, N. Krstajić, J. Monypenny, S. Coelho, D. Tyndall, R.J. Walker, V. Devauges, J. Richardson, N.Dutton, P. Barber and D. D. U. Li, "A high speed multifocal multiphoton fluorescence lifetime imaging microscope for live-cell FRET imaging," Biomed. Opt. Express **6**(2), 277-296 (2015).

[7] K. J. Gordon, V. Fernandez, P. D. Townsend, and G. S. Buller, "A shortwavelength gigahertz clocked fiber optic quantum key distribution system," IEEE J. Quantum Electron., vol. 40, no. 7, pp. 900–908, Jul. 2004.

[8] J. R. Srour and J. W. Palko, "Displacement Damage Effects in Irradiated Semiconductor Devices," *IEEE Trans. Nucl. Sci.*, vol. 60, no. 3, pp. 1740–1766, June 2013.

[9] J. R. Srour, Cheryl J. Marshall and Paul W. Marshall, "Review of Displacement Damage Effects in Silicon Devices", *IEEE Trans. Nucl. Sci.*, vol. 50, no. 3, pp. 653-670, June 203.

[10] C. Virmontois, V. Goiffon, M. S. Robbins, L. Tauziède, H. Geoffray, M. Raine, S. Girard, O. Gilard, P. Magnan, and A. Bardoux, "Dark Current Random Telegraph Signals in Solid-State Image Sensors," *IEEE Trans. Nucl. Sci.*, vol. 60 n. 6, pp. 4323-4331, Dec. 2013.

[11] F. Di Capua, M.Campajola, L. Campajola, C. Nappi, E. Sarnelli, L. Gasparini, H. Xu, "Random Telegraph Signal in Proton Irradiated Single-Photon Avalanche Diodes," IEEE Trans. Nucl. Sci., vol 65, no. 8, pp 1654-1660, August 2018.

[12] M.A. Karami, L. Carrara, C. Niclass, M. Fishburn, E. Charbon, "RTS Noise Characterization in Single-Photon Avalanche Diodes ," IEEE Trans. Nucl. Sci., vol.31, no. 7, pp. 692-694, July 2010

[13] L. Pancheri, G. Dalla Betta, L. H. C. Braga, H. Xu, D. Stoppa, "A Single-Photon Avalanche Diode test chip in 150nm CMOS technology", Microelectronic Test Structures, 2014 IEEE Conference on Microelectronic Test Structures, June 2014, 10.1109/ICMTS.2014.6841486.

[14] H. Xu, L. Pancheri, L. H. C. Braga, G. F. Dalla Betta and D. Stoppa, "Cross-talk characterization of dense single-photon avalanche diode arrays in CMOS 150-nm technology," *Optical Engineering* vol. 55 n. 067102, 2016, DOI: 10.1117/1.OE.55.6.067102

[15] H. Xu, L. H. C. Braga, D. Stoppa, L. Pancheri, "Characterization of Single-Photon Avalanche Diode Arrays in 150nm CMOS Technology", 2015 XVIII AISEM Annual Conference, pp. 1-4, 2015.

[16] Ashland™ Gafchromic radiotherapy films, Ashland Advanced Materials, Bridgewater (NJ), USA, 2017.

[17] L. Ratti, P. Brogi, G. Collazuol, G.-F. Dalla Betta, A. Ficorella, L.

Lodola, P. S. Marrocchesi, S. Mattiazzo, F. Morsani, M. Musacci, L. Pancheri, A. Savoy-Navarro, C. Vacchi, "CMOS SPAD sensors for particle tracking exposed to ionizing and non-ionizing radiation," presented at RADECS conference, Geneva, Switzerland, 2018
[18] D. R. Smith, A. D. Holland, I. B. Hutchinson, "Random telegraph signals in charge coupled devices", Nuclear Instruments & Methods in Physics Research, Section A, DOI:10.1016/j.nima.2004.03.210, Elsevier 2004.
[19] M. J. Kirton, M. J. Uren, "Noise in solid-state microstructures: a new perspective on individual defects, interface states, and low-frequency noise," Adv Phys, vol. 38, pp. 367-468, 1989.
[20] G. D. Watkins and J. W. Corbett, "Defects in irradiated silicon: electron paramagnetic resonance and electron-nuclear double resonance of the Si-E center", *Phys. Rev.,* 134 (5A), pp. 1359-1377, 1964
[21] Hopkins, I.H., Hopkinson, G.R., "Random telegraph signals from proton-irradiated CCDs," *IEEE Trans. Nucl. Sci.* vol. 40 no. 6, pp. 1567–1574, 1993.
[22] J. Bogaerts, B. Dierickx, and R. Mertens, "Random telegraph signals in a radiation-hardened CMOS active pixel sensor," *IEEE Trans. Nucl. Sci. , vol. 49, no. 1, pp. 249–257, Feb. 2002*.